NEAR SURFACE GEOSCIENCE 2015

Mo AEM 05

Geo-steered 3D Inversion of Airborne Electromagnetic Data in Rugged Terrain

C. Scholl* (CGG), J. Neumann (CGG) & M.D. Watts (CGG)

SUMMARY

Multidimensional inversions for electromagnetic (EM) data require regularization for stabilization. A common approach is to add some smoothness criterion, which provides stable results. The downside is that any feature will be uniformly blurred and tend to not appear geologically meaningful.

We present a 3D inversion algorithm for all types of airborne EM data featuring geo-steering. This additional regularization - based on a cross-gradient concept - is used to introduce assumed or known geological structures to the inversion. Using the additional information results in geologically more plausible models and increases the effective resolution of the inversion.

The approach is demonstrated with frequency domain field data set collected in rugged topography.

Introduction

Much of the quantitative interpretation of airborne electromagnetic (AEM) data sets is handled by simple 1D imaging or inversion algorithms (e.g. Vallée and Smith, 2007). Although these are fast and therefore efficient in terms of computer usage, 1D approaches do not incorporate topography and assume a horizontally-layered earth. These limitations are partially overcome by 3D inversion techniques (e.g. Cox, *et al*, 2012), but typically with apparent loss of resolution due to the requirement for regularization using a smoothing operator, as well as much increased computational costs. In this presentation, we show results of 3D standard smooth model and geo-steered inversion of a frequency domain airborne electromagnetic dataset over a massive sulphide body in Santo Domingo, verified by drill-hole data.

Modelling methodology

The 3D forward algorithms are based on a finite difference (FD) frequency domain formulation. The related equations are solved with iterative solvers using a multigrid preconditioner (Mulder, 2006). Time domain responses can also be computed using the same preconditioner for an implicit time stepping process. The inversions are smooth model inversions, where the data misfit is balanced versus model smoothness, based on a Quasi-Newton approach (Plessix and Mulder, 2008). The trade-off parameter on the smoothness terms is lowered over the course of the inversion to ultimately fit the data on average within their error estimate.

The FD grids are set up independently of the model grid, on which the inversions are carried out (Druskin and Knizhnerman, 1994; Commer, 2003; Scholl *et al*., 2004). The model grid can be unstructured in the vertical direction (Scholl and Sinkevich, 2012).

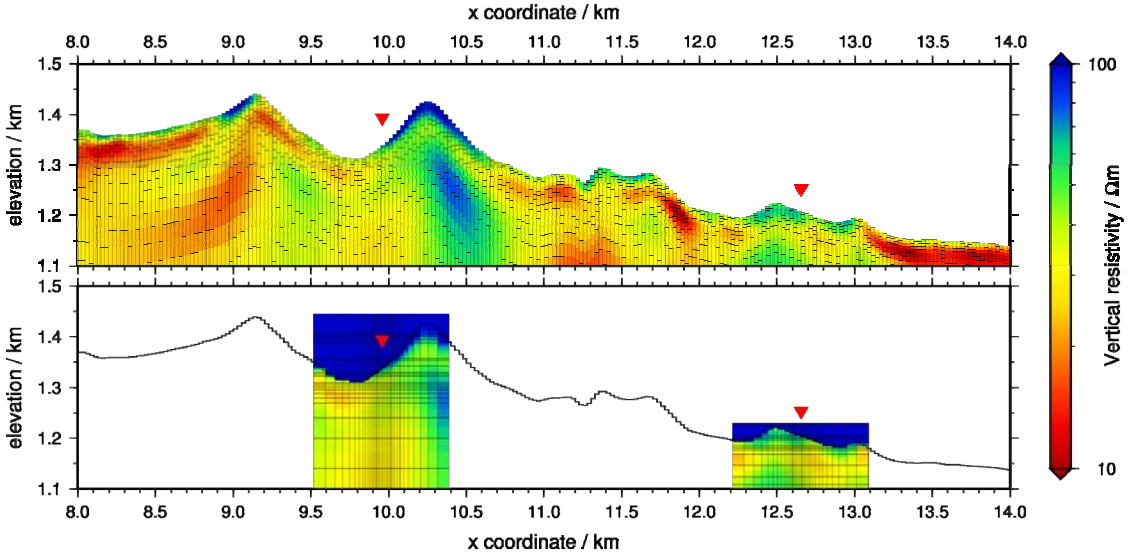

Figure 1 *Gridding example for two measurement points (red triangles, respectively); top panel shows the model cells, here draping the topography. Lower panel shows the FD grid cells for the two frequency domain systems. Levels of the FD grids containing only all-air cells are omitted.*

FD grids are set up at the start of each iteration based on the specific AEM system configuration, model resistivities and frequencies/decay times. Grid construction rules follow similar approaches to Hördt (1992) and Plessix *et al*. (2007). The model is sampled onto the FD grid cells using material averaging (e.g. in Commer and Newman, 2008). Figure 1 shows a model example and the related FD grids for two frequency domain system.

Geo-steered inversion

Inversion of AEM data is non-unique and requires additional regularization. Most commonly some sort of generic smoothing is introduced. In this example we use the regularization to steer the inversion towards a geologically plausible result using the concept of cross-gradients (Gallardo and Meju, 2003). So far, the cross-gradient approach has been used in the joint inversion of different geophysical methods. Cross-gradient regularization supports structural similarity between two otherwise independent models (for example resistivity and velocity in case of a joint inversion of DC and seismics).

Our approach is to use cross-gradients to steer the inversion towards structural similarity to a model built based on geological a priori knowledge such as dips. The basic idea is that the gradients of the inversion model (e.g. resistivity) should be parallel or anti-parallel to some other set of gradients. This is achieved by adding another regularization term which is the vector product of the two gradients; this works because the norm of the vector product of two vectors is zero if the vectors are parallel or antiparallel. The term defines only the direction of a change; it will not define if the model values should increase or decrease in that direction. It also will not say anything about the strength of the change, so arbitrary numerical values can be used to set up the steering model.

Input data

The survey area, a rugged sector of the Cordillera Central of San Domingo, covered a sequence of Cretaceous metavolcanics with a known volcanogenic massive sulfide deposit (Roos *et al*., 2007). Frequency domain EM data were collected in 2007 using the DIGHEM^{V} system (Fraser, 1972), at a nominal height of 40 m above ground level. The frequency range employed was 915 to 56khz, with data from all 5 coil pairs being used (two coaxial, three coplanar). The data were down-sampled to 15 m. Altimeter and vertical position data from the survey were used as topography for the model.

Inversion

Previous inversion work (Smith and Hodges, 2008) showed 1D results along the southernmost survey line (Figure 2). Although the position of the conductive orebody is identified, the strongly 3D nature of the target results in a distorted image.

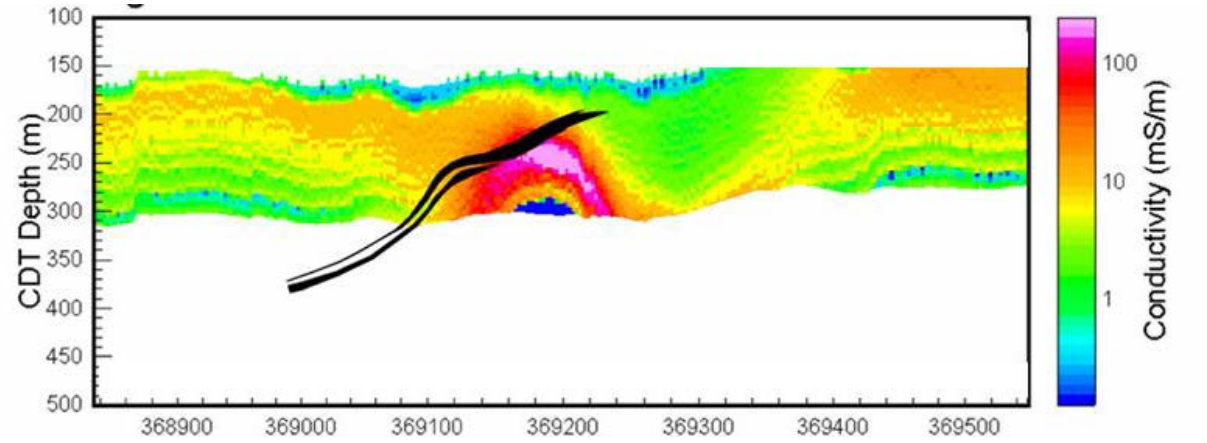

Figure 2 *1D conductivity section across the Maimon orebody (fig. 4 from Smith and Hodges, 2008).*

For geo-steering of the 3D inversion, we used regional dips from Roos *et al*. (2007). Those were introduced into the inversion by setting up a model of arbitrary numerical values with a dip of 45 degrees (Figure 3, left). The inversion is set up to produce a smooth model which predominantly exhibits resistivity gradients parallel or antiparallel to the steering model. The inversion result defines a SW-dipping conductor (Figure 3, right, and Figure 4, left), plunging to the SE. This may be compared with the conventionally-regularized inversion shown in the right panel of Figure 4.

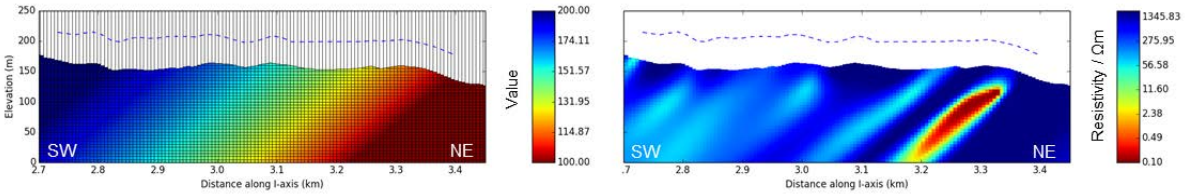

Figure 3 *SW-NE sections of the 3D model along line 13515; geo-steering model used for geo-steering (left) and 3D inversion result (right).*

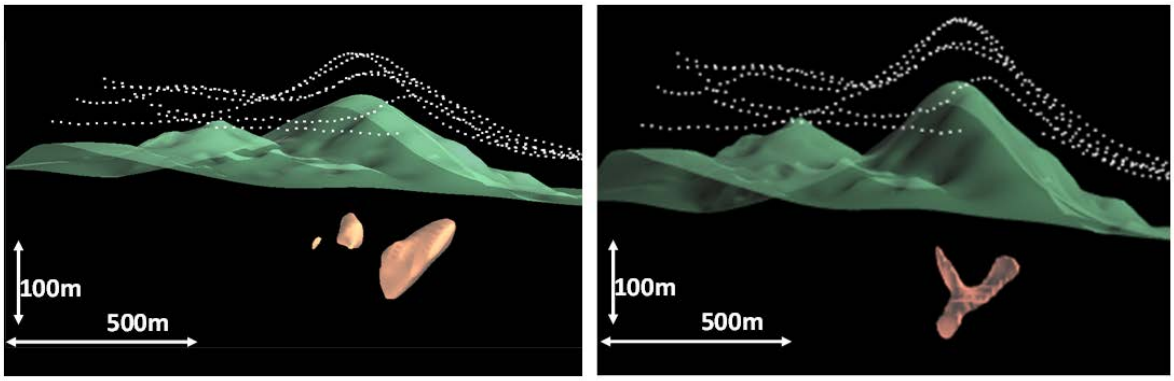

Figure 4 *The Maimon conductive body as imaged by 3D geosteered (left) or standard regularized (right) inversion, showing resistivity <1 ohm.m. White dots show the flight path; topography from airborne survey data.*

Comparison with geology

Roos *et al*. (2007) show dip and strike sections of the orebody, reproduced below in Figure 5. These are in good agreement with the 3D conductor imaged by inversion.

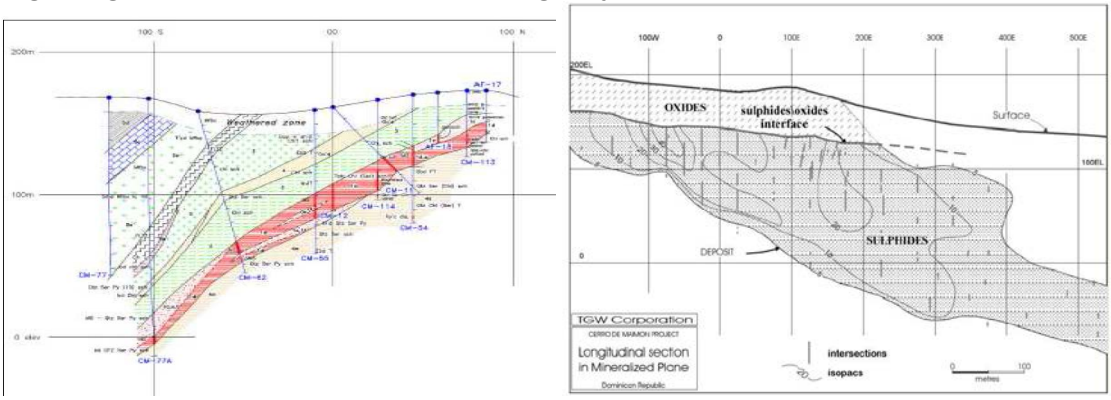

Figure 5 *Section through the Maimon orebody; left: NW-looking section with the body in red; right: NE-looking (strike) section.*

Conclusions

We have developed a method to steer the inversion of AEM data in complex topographic and geologic environments using a simple structural reference model. In the case illustrated here, the use of regional geological dips has notably increased the geological plausibility over blind, unconstrained inversion approaches. Used in conjunction with both the computation of the complete earth response from fully 3D inversion, including detailed topography, and the efficient computation times through the multi grid formulation employed, accurate and geologically reasonable depth inversion solutions are now available for all airborne EM datasets. Integrating ancillary information in this way can thus increase the effective resolution significantly. The same approach, naturally, can be extended to other

types of observed and reference data, for example airborne gravity and gradiometry, plus migrated seismic data, and to the Marine and Land environments.

Acknowledgements

Geological sections are shown by courtesy of Globestar Mining Corporation; Greg Hodges of CGG Toronto is thanked for the AEM data.

References

Commer M. [2003] Three-dimensional inversion of transient electromagnetic data: A comparative study. *Mitteilungen aus dem Institut für Geophysik und Meteorologie der Universitaet zu Köln*, **157**.

Commer M. and Newman G.A. [2008] New advances in three-dimensional controlled-source electromagnetic inversion. *Geophys. J. Int.*, **172**, 513-535.

Cox, L.H., Wilson, G.A., and Zhdanov, M.S. [2012] 3D inversion of airborne electromagnetic data. *Geophysics*, **77**(4), WB59-WB69.

Druskin, V. and Knizhnerman, L. [1994] Spectral approach to solving three-dimensional Maxwell's diffusion equations in the time in the time and frequency domain. *Radio Science*, **29**, 937-953.

Gallardo, L.A. and Meju, M.A. [2003] Characterization of heterogeneous near-surface materials by joint 2D inversion of dc resistivity and seismic data. *Geophys. Res. Lett.*, **30**, 1658.

Fraser, D.C. [1972] A new multicoil aerial electromagnetic prospecting system. *Geophysics*, **37**, 518-537.

Hördt, A. [1992] Interpretation transient elektromagnetischer Tiefensondierungen für anisotropy horizontal geschichtete und für dreidimensionale Leitfähigkeitstrukturen. *Mitteilungen aus dem Institut für Geophysik und Meteorologie der Universitaet zu Köln*, **86**.

Mulder, W.A. [2006] A multigrid solver for 3D electromagnetic diffusion, *Geophys. Prosp*., **54**, 633-649.

Plessix, R.-E. and Mulder, W.A. [2008] Resistivity imaging with controlled-source electromagnetic data: depth and data weighting. *Inverse Problems*, **24**, doi:10.1088/0266-5611/24/3/034012.

Roos, P., Burgess, H. and Ward, I. [2007] Updated Mineral Resource And Reserve Estimate, Cerro De Maimón Project, Msnr. Nouel Province, Dominican Republic. *Technical Report NI 43-101 for GlobeStar Mining Corporation*.

Scholl C., R. Martin, O. Koch, S. L. Helwig, B. Tezkan, DESERT research group [2004] 2.5-D inversion of transient electromagnetic data. *Abstracts of the 17th International Workshop on Electromagnetic Induction in the Earth, Hyderabad, India*.

Scholl C. and Sinkevich, V.A. [2012] Modeling mCSEM data with a finite difference approach and an unstructured model grid in the presence of bathymetry. *Abstracts of the 21st EM Induction Workshop, Darwin, Australia*.

Smith, R., and Hodges, G. [2008] The HeliGEOTEMsystem, with an example of data from the Maimon deposit in the Dominican Republic. *Proceedings of AEM2008 – 5th International Conference on Airborne Electromagnetic, Finland 28-30 May 2008*.

Vallée, M., and R. Smith [2007] Comparison of fixed-wing airborne electromagnetic 1D inversion methods. *Proceedings of Exploration 07: 5th Decennial International Conference on Mineral Exploration*, 1067-1072.